

Hydrothermally Stable $\text{WO}_3/\text{ZrO}_2\text{-Ce}_{0.6}\text{Zr}_{0.4}\text{O}_2$ Catalyst for the Selective Catalytic Reduction of NO with NH_3

Tinku Baidya · Andreas Bernhard ·
Martin Elsener · Oliver Kröcher

Published online: 22 February 2013
© Springer Science+Business Media New York 2013

Abstract A new catalyst $\text{WO}_3/\text{ZrO}_2\text{-Ce}_{0.6}\text{Zr}_{0.4}\text{O}_2$ (15 wt % $\text{WO}_3/\text{ZrO}_2\text{:Ce}_{0.6}\text{Zr}_{0.4}\text{O}_2 = 50:50$) has been developed for the selective catalytic reduction of NO with NH_3 . The redox component $\text{Ce}_{0.6}\text{Zr}_{0.4}\text{O}_2$ was dispersed on the surface of acidic WO_3/ZrO_2 by the solution combustion method showing the best NO_x reduction efficiency among the catalysts prepared by various modes of mixing of the components. The catalyst has been characterized by XRD, Raman spectroscopy and $\text{NH}_3\text{-TPD}$. A NO_x reduction efficiency of more than 90 % was obtained between 300 and 500 °C at $\alpha = \text{NH}_{3,\text{in}}/\text{NO}_{x,\text{in}} = 1$. The catalyst showed stable NO_x reduction efficiency after hydrothermal ageing at 700 °C. Sulfur poisoning promoted the NO_x reduction efficiency at high temperatures at the expense of a reduced activity at lower temperatures, but the catalyst could be fully regenerated by heating in O_2 at 650 °C.

Keywords Selective catalytic reduction · SCR · Catalyst · Rare earth metal oxides

1 Introduction

NO_x abatement from diesel engine exhaust is one of the major challenges in environmental catalysis. NO_x gases are the major source of pollution and photochemical smog formation. The most efficient technology to remove NO_x from stationary sources is the selective catalytic reduction (SCR) of NO_x by ammonia ($4\text{NH}_3 + 4\text{NO} + \text{O}_2 \rightarrow 4\text{N}_2 + 6\text{H}_2\text{O}$) [1–4]. Reduction of NO_x from diesel engine emissions

requires a highly efficient catalyst operating over a temperature range of 200–500 °C at high space velocity. Under certain circumstances such as diesel particulate filter (DPF) regeneration, the diesel exhaust gas temperature can even go up to slightly above 700 °C [5]. For light-duty vehicles its use is restricted by the complexity and large dimensions of the SCR system that must incorporate also a tank for the aqueous urea solution (NH_3 precursor), a urea hydrolysis catalyst and eventually an NH_3 slip catalyst [6]. Other critical aspects are the limited hydrothermal stability and the potentially toxic emissions of currently available SCR catalysts [7–9].

Among metal oxide-based SCR catalysts, commercially used $\text{V}_2\text{O}_5/\text{WO}_3\text{-TiO}_2$ catalysts are highly active, but serious concern exists with respect to high temperature stability and sensitivity to phosphorus [2]. Manganese based catalysts also works very well at low temperature, but NO conversion is decreased significantly above 350 °C [10–18] and they easily deactivate by sulfur.

Recently, ceria-based SCR catalysts have attracted much attention due to their advantageous redox properties [14–23] and ceria-promoted acidic zirconia systems seem to be particularly attractive [24]. For instance, by using $\text{Ce}_{1-x}\text{Zr}_x\text{O}_2$ as redox component NO_x reduction efficiency is maximized [19] and hydrothermal stability may be further enhanced by dispersing on a stable high surface acidic oxide. The activity is further enhanced by the addition of acidic components to bind ammonia, such as vanadate, tungstate or niobate [19, 22, 25]. However, the acidic component dispersed on the metal oxide surface tends to separate out under hydrothermal ageing at high temperatures initiated by sintering of the surface. Tungstate (WO_3) is not only useful as acidic component but can also function as stabilizer for the underlying metal oxide. It has been found, for example, that a layer of WO_3 stabilizes anatase

T. Baidya · A. Bernhard · M. Elsener · O. Kröcher (✉)
Paul Scherrer Institut, OVGA/112, 5232 Villigen PSI,
Switzerland
e-mail: oliver.kroecher@psi.ch

TiO₂ and vice versa at temperatures up to 800 °C. Similarly, WO₃ dispersed on ZrO₂ may keep the tungstate species stable and, consequently, preserve the amount of acidic sites at the surface. If WO₃/ZrO₂ and CeO₂-ZrO₂ are combined, Ce_{1-x}Zr_xO₂ may disperse on the high surface WO₃/ZrO₂ thereby maximizing the NO_x reduction efficiency and preventing the loss of redox activity of Ce_{1-x}Zr_xO₂ due to sintering of the surface at high temperatures.

In this paper, we report a new mixed phase oxide catalyst, 15 wt % WO₃/ZrO₂-Ce_{1-x}Zr_xO₂ that shows high NO_x reduction efficiency with NH₃. The catalyst was characterized by XRD and NH₃-TPD techniques. The catalyst performance was tested under various conditions including tests with urea solution, representative for SCR systems aboard of diesel vehicles.

2 Experimental

2.1 Catalysts Preparation and Characterization

The catalysts were prepared following different methods including the solution combustion method [26] and incipient wetness impregnation. 15 wt % WO₃/ZrO₂-Ce_{0.6}Zr_{0.4}O₂ was made in two steps as following.

In the first step, 15 wt % WO₃/ZrO₂ was prepared by dissolving ammonium tungstate in a NH₃ solution and adding ZrO₂. The suspension was evaporated to dryness. The solid was dried in air at 120 °C for 6 h and then calcined at 650 °C for 5 h.

In the second step, 15 wt % WO₃/ZrO₂ was mixed with the other component Ce_{0.6}Zr_{0.4}O₂ by two different methods. This was done a) by forming Ce_{0.6}Zr_{0.4}O₂ phase directly in presence of WO₃/ZrO₂ suspended in a Ce and Zr precursor solution, or b) by ball milling of a mixture of 15 wt % WO₃/ZrO₂ and Ce_{0.6}Zr_{0.4}O₂ phases in a 50:50 ratio.

The first method a) of preparation could be accomplished by solution combustion method as well as co-precipitation method, commonly called CP catalysts. In the solution combustion method, an aqueous solution of (NH₄)₂Ce(NO₃)₆, ZrO(NO₃)₂ and C₂H₅NO₂ (fuel) was prepared in the molar ratio 0.6:0.4:0.51. 15 wt % WO₃/ZrO₂ was added to the solution forming a suspension solution and kept at 400 °C in the furnace. After evaporation at the point of complete drying the mixture ignited and the combustion product was obtained in a minute. In this preparation method, ¼ of the stoichiometrically calculated amount of fuel was used to avoid formation of voluminous oxides. This sample was marked SCM. In the co-precipitation method, the hydroxides were precipitated from a solution of ZrO(NO₃)₂ and (NH₄)₂Ce(NO₃)₆ and stirred for 6 h for homogeneous mixing. Then, 15 wt % WO₃/ZrO₂ was added to the hydroxides suspension and the

resulting mixture was stirred until complete evaporation. The precipitate was dried at 120 °C for 3 h and then calcined at 650 °C for 5 h. The samples obtained by using this method was marked 'Co-prep'.

In the second method b), the Ce_{0.6}Zr_{0.4}O₂, used in the ball milling (BM) mixing, was also prepared by both solution combustion as well as co-precipitation method as described above and was marked by the same abbreviations SCM and Co-prep, respectively.

10 wt % WO₃/Ce_{0.6}Zr_{0.4}O₂ was prepared by the wet impregnation method. Ammonium tungstate was dissolved in an ammonia solution and added to Ce_{0.6}Zr_{0.4}O₂ such that it just wets the oxides. The resulting product was dried in air at 120 °C for 3 h and calcined at 650 °C for 5 h. This sample was marked IMP.

The catalysts were coated on cordierite honeycombs following previous described methods [8]. The catalyst loading was ~200 mg/cc.

X-ray diffraction measurements were carried out on a Bruker D8 Advance diffractometer using Cu K_α radiation. The XRD patterns were collected over the 2θ range of 20° to 70° at a step size of 0.01°. To minimize the influence of texture, the samples were rotated during each measurement.

Ammonia Temperature-Programmed Desorption (NH₃-TPD) was applied to measure the surface acidity of the materials and check their NH₃ storage capacities (ASC, expressed in mL/g). For this purpose, 200 mg powder catalyst were placed in a quartz U-shaped down-flow reactor (total length: 150 mm; internal diameter: 8 mm). The temperature was measured with a thermocouple located inside the reactor. In a first step, the sample was pre-treated in a flow of 30 mL/min He at 500 °C for 30 min. Ammonia adsorption was carried out for 15 min at 50 °C using a flow of 30 mL/min of 5 vol. % NH₃/He. After purging at 50 °C for 1 h with pure He, the desorption of NH₃ was monitored with a Thermal Conductivity Detector (TCD) during heating up to 650 °C with 10 K/min.

2.2 Catalytic Activity Tests

The NO SCR activity with NH₃ gas was tested between 200 and 550 °C by feeding 1000 ppm NO, 1000 ppm NH₃, 10 % O₂, 5 % H₂O and N₂ into a quartz plug-flow reactor at a gas hourly space velocities (GHSV) of 50,000 h⁻¹. The resulting NO, NO₂, N₂O and unreacted NH₃ were quantified with a Nicolet Magna-IR 560 FTIR spectrometer [8]. The NO_x reduction efficiency (DeNO_x) was calculated as follows:

$$\text{DeNO}_x(\%) = \frac{\text{NO}_{x,\text{in}} - \text{NO}_{x,\text{out}}}{\text{NO}_{x,\text{in}}} \times 100$$

where NO_x is the sum of NO and NO_2 concentrations.

Besides the equimolar dosage of NO_x and NH_3 , the NH_3 concentration was gradually increased from 100 to 1500 ppm at a constant NO concentration of 1000 ppm for assessing the ammonia slip of the catalyst (surface acidity), its redox potential and its ammonia oxidation potential.

3 Results and Discussions

The catalyst contains 15 wt % WO_3/ZrO_2 as acid and $\text{Ce}_{1-x}\text{Zr}_x\text{O}_2$ as redox component. To find the best composition regarding x , the NO SCR activity over 15 wt % $\text{WO}_3/\text{ZrO}_2\text{-Ce}_{1-x}\text{Zr}_x\text{O}_2$ was tested with $x = 0.0\text{--}0.5$. The reference material 10 wt % $\text{WO}_3/\text{ZrO}_2\text{-CeO}_2$ showed high NO_x reduction efficiency at all temperatures. The NO_x reduction efficiency over the $\text{WO}_3/\text{ZrO}_2\text{-Ce}_{1-x}\text{Zr}_x\text{O}_2$ catalysts did not change much with increasing Zr concentration from $x = 0.0$ to 0.5 , except slightly lower NO_x conversion at high temperatures. At high temperatures, slightly more NH_3 oxidation occurred for higher Zr contents up to $x = 0.4$. At $x = 0.5$, a lower activity was observed at lower temperatures. Therefore, since the optimum Zr content also enhances both the redox activity and the hydrothermal stability, we choose $\text{Ce}_{0.6}\text{Zr}_{0.4}\text{O}_2$ ($x = 0.4$) as composition for the redox component in the target catalyst.

The mode of mixing of the components in the catalyst may change the NO_x reduction efficiency. It can be done in two ways: as prepared $\text{Ce}_{0.6}\text{Zr}_{0.4}\text{O}_2$ can be added to WO_3/ZrO_2 and then mixed by ball milling (marked BM) or $\text{Ce}_{0.6}\text{Zr}_{0.4}\text{O}_2$ can be crystallized directly from the precursors on the WO_3/ZrO_2 surface (marked CP). Figure 1 shows a comparison of the NO_x reduction efficiency over these catalysts of the common formula 15 wt % $\text{WO}_3/\text{ZrO}_2\text{-Ce}_{0.6}\text{Zr}_{0.4}\text{O}_2$. Ball milling of WO_3/ZrO_2 and $\text{Ce}_{0.6}\text{Zr}_{0.4}\text{O}_2$ resulted in a much lower activity as compared to the later method. The $\text{Ce}_{0.6}\text{Zr}_{0.4}\text{O}_2$ component in BM and CP catalysts could be prepared by both the solution combustion method and the co-precipitation method. Obviously, the CP catalysts were generally more active than the BM catalysts. In the BM catalysts, when $\text{Ce}_{0.6}\text{Zr}_{0.4}\text{O}_2$ was prepared by the co-precipitation method (Co-prep), it showed a higher NO_x reduction efficiency than the same catalyst with $\text{Ce}_{0.6}\text{Zr}_{0.4}\text{O}_2$ prepared by solution combustion (SCM). Although WO_3/ZrO_2 was the common component used in all catalyst preparations, the close proximity of redox sites and acidic sites in the CP catalysts seems to be decisive to achieve high NO_x reduction efficiency. It seems to be reasonable to assume that $\text{Ce}_{0.6}\text{Zr}_{0.4}\text{O}_2$ crystallites could form on the surface and were distributed more homogeneously in the CP catalysts.

Since the CP catalyst from solution combustion was the easiest to prepare, we continued with this type for the further studies. The potential formation of a $\text{Ce}_{0.6}\text{Zr}_{0.4}\text{O}_2$ solid solution on the WO_3/ZrO_2 surface in the 10 wt % $\text{WO}_3/\text{ZrO}_2\text{-Ce}_{0.6}\text{Zr}_{0.4}\text{O}_2$ (SCM) catalyst was examined by XRD in Fig. 2. For the purpose of comparison of the peak positions in the mixed oxides, pure $\text{Ce}_{0.6}\text{Zr}_{0.4}\text{O}_2$ phase and 10 wt % $\text{WO}_3/\text{ZrO}_2\text{-Ce}_{0.6}\text{Zr}_{0.4}\text{O}_2$ (Co-prep) are also shown in Fig. 2. To identify the phases present in the mixed

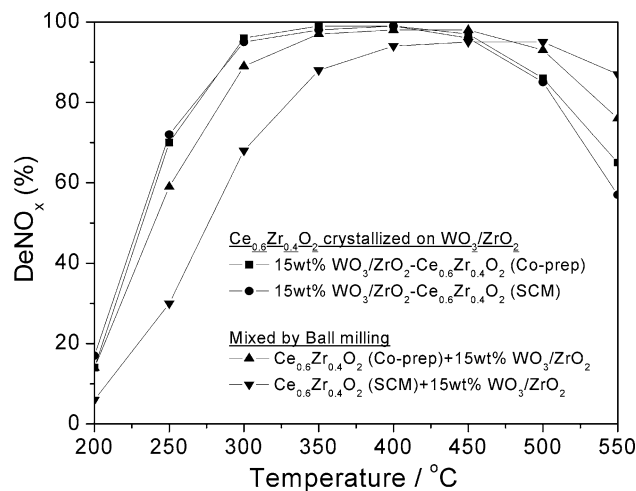


Fig. 1 NO_x reduction efficiency over various 15 wt % $\text{WO}_3/\text{ZrO}_2\text{-Ce}_{0.6}\text{Zr}_{0.4}\text{O}_2$ prepared by different way of mixing the components, i.e., 15 wt % WO_3/ZrO_2 and $\text{Ce}_{0.6}\text{Zr}_{0.4}\text{O}_2$. Model gas: 1000 ppm NO , 1000 ppm NH_3 , 10 % O_2 , 5 % H_2O and N_2 at $\text{GHSV} = 50,000 \text{ h}^{-1}$

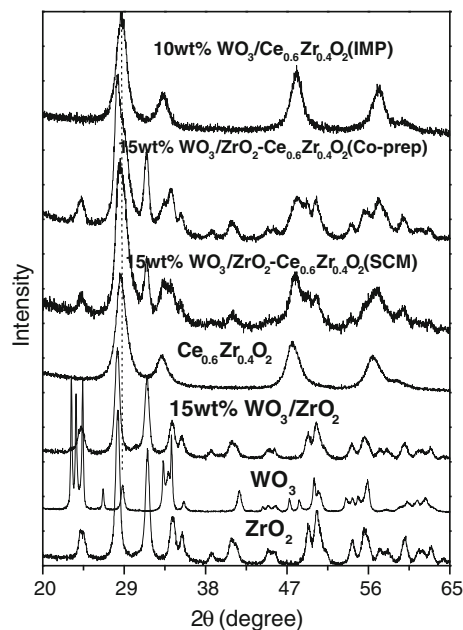


Fig. 2 X-ray diffraction profile of ZrO_2 , WO_3 , 15 wt % WO_3/ZrO_2 , $\text{Ce}_{0.6}\text{Zr}_{0.4}\text{O}_2$, 15 wt % $\text{WO}_3/\text{ZrO}_2\text{-Ce}_{0.6}\text{Zr}_{0.4}\text{O}_2$ (SCM), 15 wt % $\text{WO}_3/\text{ZrO}_2\text{-Ce}_{0.6}\text{Zr}_{0.4}\text{O}_2$ (Co-prep) and 10 wt % $\text{WO}_3/\text{Ce}_{0.6}\text{Zr}_{0.4}\text{O}_2$ (IMP)

oxides, the characteristic reflections from pure ZrO_2 and WO_3 are also shown. Both ZrO_2 and WO_3 remained in the monoclinic structure after calcination at 650°C . Although, the presence of these oxides were expected in the mixed oxide catalyst there is no reflection at 23° , excluding the presence of WO_3 crystallites in WO_3/ZrO_2 and indicating finely dispersed WO_3 on the ZrO_2 surface. $\text{Ce}_{0.6}\text{Zr}_{0.4}\text{O}_2$ on the WO_3/ZrO_2 surface in the 15 wt % $\text{WO}_3/\text{ZrO}_2\text{-Ce}_{0.6}\text{Zr}_{0.4}\text{O}_2$ (SCM) catalyst could not be detected because the peaks were overlapped with the ZrO_2 peak. It is clearly visible that the peaks of 15 wt % $\text{WO}_3/\text{ZrO}_2\text{-Ce}_{0.6}\text{Zr}_{0.4}\text{O}_2$ (SCM) are broader than of the 15 wt % $\text{WO}_3/\text{ZrO}_2\text{-Ce}_{0.6}\text{Zr}_{0.4}\text{O}_2$ (Co-prep) catalyst indicating a smaller crystallite size in the SCM catalyst. The main peak in 15 wt % $\text{WO}_3/\text{ZrO}_2\text{-Ce}_{0.6}\text{Zr}_{0.4}\text{O}_2$ (Co-prep) becomes unsymmetrical due to an overlap with the ZrO_2 peak. Note that the relative intensity of the peaks remained the same confirming a homogeneous distribution of $\text{Ce}_{0.6}\text{Zr}_{0.4}\text{O}_2$. The formation of $\text{Ce}_{0.6}\text{Zr}_{0.4}\text{O}_2$ was confirmed by the shift of the Raman band at around 455 cm^{-1} with respect to CeO_2 .

NH_3 TPD was used to determine the surface acidity which is required to bind ammonia at the surface as a condition for high NO_x reduction efficiencies. Figure 3 shows the NH_3 desorption profiles over $\text{Ce}_{0.6}\text{Zr}_{0.4}\text{O}_2$, 15 wt % WO_3/ZrO_2 and 15 wt % $\text{WO}_3/\text{ZrO}_2\text{-Ce}_{0.6}\text{Zr}_{0.4}\text{O}_2$. Pure $\text{Ce}_{0.6}\text{Zr}_{0.4}\text{O}_2$ desorbs weakly adsorbed NH_3 below 350°C . Since the WO_3/ZrO_2 surface is strongly acidic, the NH_3 desorption tail goes up to 600°C in 15 wt % WO_3/ZrO_2 . A similar type of acidic sites is also present in 15 wt % $\text{WO}_3/\text{ZrO}_2\text{-Ce}_{0.6}\text{Zr}_{0.4}\text{O}_2$ as evident from the desorption profile.

Figure 4a shows the NO_x reduction efficiency of the most promising catalyst 15 wt % $\text{WO}_3/\text{ZrO}_2\text{-Ce}_{0.6}\text{Zr}_{0.4}\text{O}_2$ with varying space velocity from 20,000 to 50,000 h^{-1} . Even at the highest space velocity of 50,000 h^{-1} almost

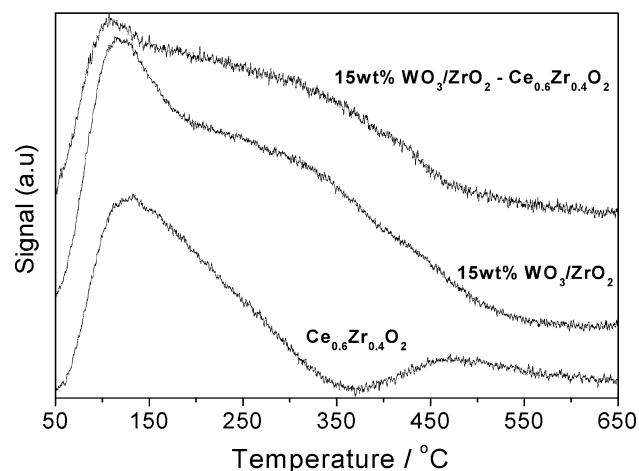


Fig. 3 NH_3 -TPD over $\text{Ce}_{0.6}\text{Zr}_{0.4}\text{O}_2$, 15 wt % WO_3/ZrO_2 and 15 wt % $\text{WO}_3/\text{ZrO}_2\text{-Ce}_{0.6}\text{Zr}_{0.4}\text{O}_2$

full conversion was measured between 300 to 550°C . Only below 300°C , a significant decrease in activity was observed with increasing space velocity. At low temperatures, the reaction rate became slow because the redox activity of CeO_2 significantly decreased. Figure 4b shows the NO_x reduction efficiency (DeNO_x) of this catalyst versus NH_3 slip. This plot demonstrates that DeNO_x is high at 10 ppm NH_3 emissions above 300°C . Moreover, the steeply rising curves confirm the high surface acidity of the catalyst, because already at rather low NH_3 dosage the local NH_3 concentration at the SCR sites are high enough to reach almost the maximum activity of the catalyst.

Figure 5 shows a comparison between the 15 wt % $\text{WO}_3/\text{ZrO}_2\text{-Ce}_{0.6}\text{Zr}_{0.4}\text{O}_2$ catalyst and a commercial vanadium-based reference catalyst. It is obvious that there was no significant difference in NO_x reduction efficiency in the

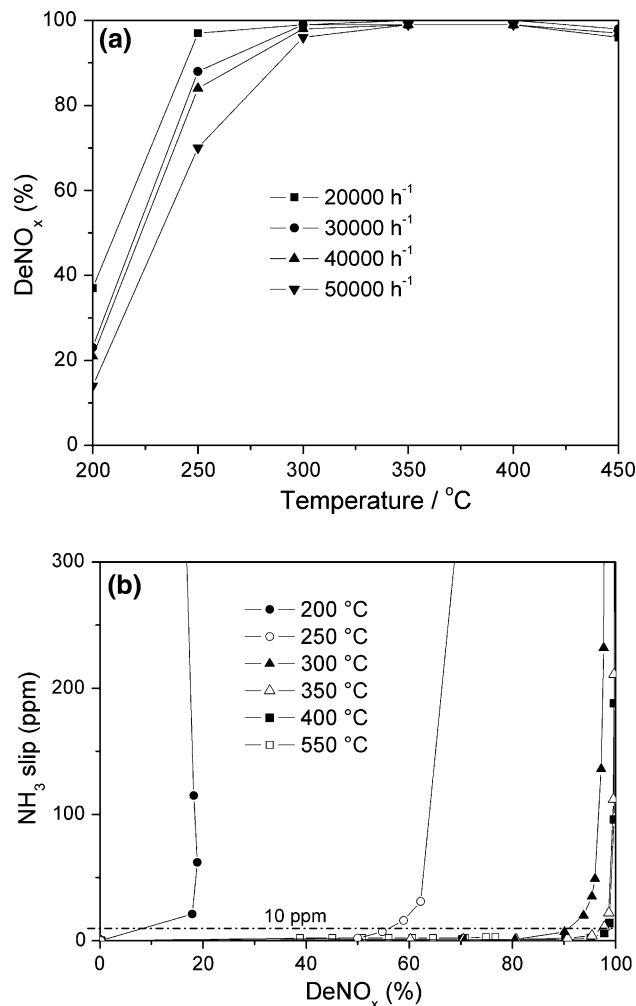


Fig. 4 **a** NO_x reduction efficiency (DeNO_x) vs temperature over 15 wt % $\text{WO}_3/\text{ZrO}_2\text{-Ce}_{0.6}\text{Zr}_{0.4}\text{O}_2$ with varying space velocity. **b** NH_3 slip vs DeNO_x over 15 wt % $\text{WO}_3/\text{ZrO}_2\text{-Ce}_{0.6}\text{Zr}_{0.4}\text{O}_2$. Model gas: 1000 ppm NO , 200–1500 ppm NH_3 , 10 % O_2 , 5 % H_2O and N_2 as balance

temperature range from 250 to 550 °C. The reference catalyst produced much higher amounts of N₂O above 450 °C compared to the 15 wt % WO₃/ZrO₂-Ce_{0.6}Zr_{0.4}O₄ catalyst, which on the other side produced slightly more N₂O at lower temperatures. The 10 wt % WO₃/Ce_{0.6}Zr_{0.4}O₂ catalyst, which was included in Fig. 5 for the purpose of comparison, showed a similar NO_x reduction efficiency in the fresh state.

However, after hydrothermal aging substantial differences between these two catalysts became apparent, which are presented in Fig. 6. Hydrothermal ageing was performed successively at 675, 700 and 750 °C. The NO_x reduction efficiency of the 15 wt % WO₃/ZrO₂-Ce_{0.6}Zr_{0.4}O₂ catalyst remained almost unchanged over the

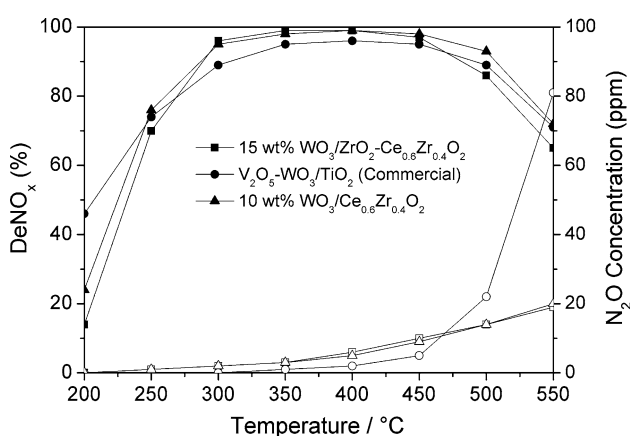


Fig. 5 A comparison of NO_x reduction efficiency between 15 wt % WO₃/ZrO₂-Ce_{0.6}Zr_{0.4}O₂ and reference catalysts V₂O₅-WO₃/TiO₂ and 10wt % WO₃/Ce_{0.6}Zr_{0.4}O₂. Model gas: 1000 ppm NO, 1000 ppm NH₃, 10 % O₂, 5 % H₂O and N₂ at GHSV = 50,000 h⁻¹

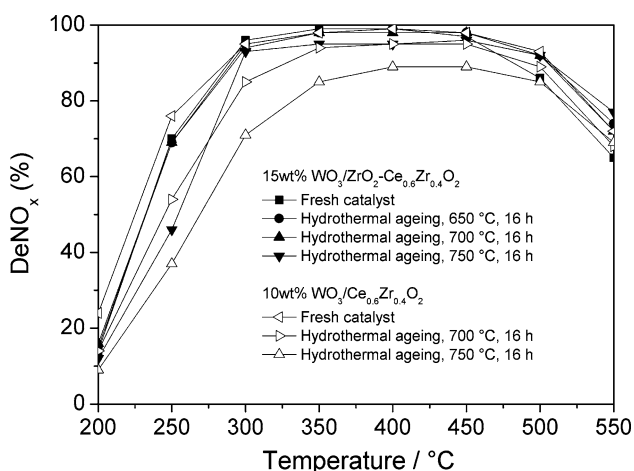


Fig. 6 NO_x reduction efficiency (closed symbols) and N₂O emissions (open symbols) vs temperature of fresh and hydrothermally aged 15 wt % WO₃/ZrO₂-Ce_{0.6}Zr_{0.4}O₂ sample and 10 wt % WO₃/Ce_{0.6}Zr_{0.4}O₂. Model gas: 1000 ppm NO, 1000 ppm NH₃, 10 % O₂, 5 % H₂O and N₂ at GHSV = 50,000 h⁻¹

entire temperature range after hydrothermal treatment up to 700 °C. At 750 °C, there was some deactivation in activity mainly below 300 °C. Hydrothermal ageing of the 10 wt % WO₃/Ce_{0.6}Zr_{0.4}O₂ catalyst started to decrease the NO_x reduction efficiency significantly even at 700 °C and it went further down at 750 °C. The hydroxyl groups on the monoclinic ZrO₂ surface might be responsible for the observed differences by forming stronger bonds with WO₃ species than with the surface of Ce_{0.6}Zr_{0.4}O₂. Since WO₃/ZrO₂ is more stable than WO₃ alone, Ce_{0.6}Zr_{0.4}O₂ remains dispersed avoiding the loss of active sites.

The effect of SO₂ on the NO_x reduction efficiency of the 10 wt % WO₃/ZrO₂-Ce_{0.6}Zr_{0.4}O₂ catalyst is presented in Fig. 7. After 5 h of SO₂ dosing, a promoting effect on the NO_x reduction efficiency was observed at high temperatures, whereas the activity was decreased below 300 °C. At 550 °C, the NO_x reduction efficiency increased from 65 to 76 %, while it decreased from 71 % to 46 % at 250 °C. The catalyst could be regenerated after heating in O₂ at 650 °C. The increase in activity at high temperatures could be due to an increase in acidity by the presence of sulfate groups. The presence of sulfate groups avoided ammonia oxidation leading to higher NO_x reduction efficiencies at high temperature, while the surface coverage with sulfate reduced the redox property decreasing the NO_x reduction efficiency at lower temperatures.

Figure 8 compares the SCR activity of 15 wt % WO₃/ZrO₂-Ce_{0.6}Zr_{0.4}O₄ with NH₃ gas and urea solution as reducing agents in the same reactor at 200, 250, 275 and 300 °C. The NH₃ slip-DeNO_x curves show an identical behavior. The NO_x reduction efficiency with urea solution was somewhat lower for some measurement points because Al₂O₃ had to be added as catalyst binder in this experiment. This means that urea hydrolysis was also efficiently

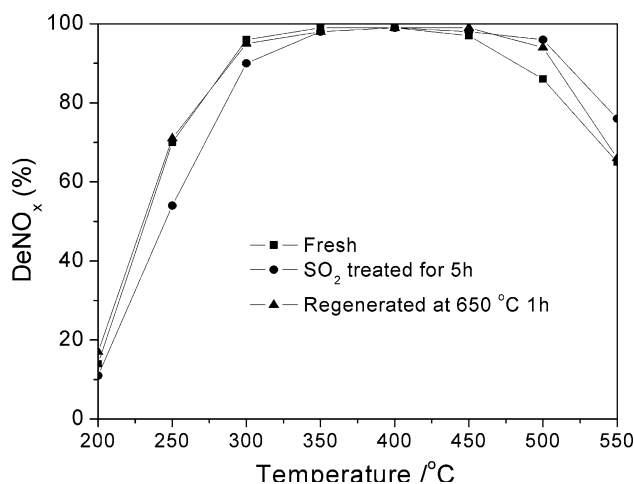


Fig. 7 SCR activities of the fresh and 5 h SO₂-poisoned and reactivated 15 wt % WO₃/ZrO₂-Ce_{0.6}Zr_{0.4}O₂. Model gas: 1000 ppm NO, 1000 ppm NH₃, 10 % O₂, 5 % H₂O and N₂ at GHSV = 50,000 h⁻¹

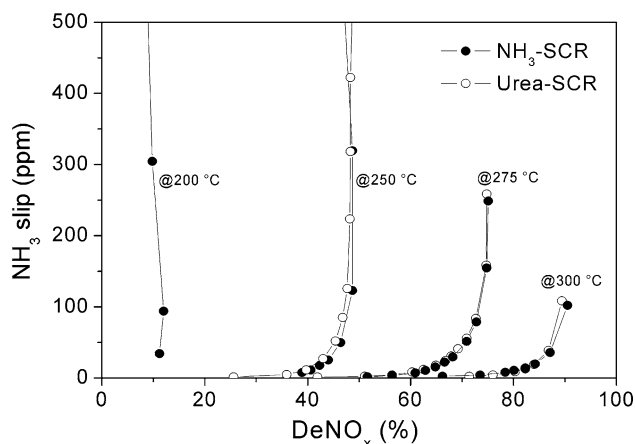


Fig. 8 NH_3 slip versus DeNO_x during urea and NH_3 SCR over 15wt % $\text{WO}_3/\text{ZrO}_2\text{-Ce}_{0.6}\text{Zr}_{0.4}\text{O}_2$. Model gas: 1000 ppm NO , 1000 ppm NH_3 (or the corresponding amount of urea), 10 % O_2 , 5 % H_2O and N_2 at $\text{GHSV} = 50,000 \text{ h}^{-1}$

catalyzed, which renders the catalyst suitable for both stationary application with NH_3 gas and mobile applications with urea solution.

4 Conclusion

$\text{Ce}_{0.6}\text{Zr}_{0.4}\text{O}_2$ was grown on 15 wt % WO_3/ZrO_2 yielding a highly stable 15 wt % $\text{WO}_3/\text{ZrO}_2\text{-Ce}_{0.6}\text{Zr}_{0.4}\text{O}_2$ catalyst for the SCR process with NH_3 and urea. The catalyst activity was completely unaffected by hydrothermal aging up to 700 °C. The SO_2 treatment had only a limited effect on the SCR activity and the sample could be regenerated fully at 650 °C. The most important result regarding the application was that the CeO_2 content in the catalyst could be reduced by 50 % by dispersing $\text{Ce}_{0.6}\text{Zr}_{0.4}\text{O}_2$ on WO_3/ZrO_2 , which kept the NO_x reduction efficiency at a similar level as the 10 wt % $\text{WO}_3/\text{Ce}_{0.6}\text{Zr}_{0.4}\text{O}_2$ reference catalyst.

References

- Gabrielsson PLT (2004) *Top Catal* 28:177
- Koebel M, Elsener M, Kleemann M (2000) *Catal Today* 59:335
- Forzatti P (2001) *Appl Catal A* 222:221
- Centi G, Perathoner S (2007) *Stud Surf Sci Catal* 171:1
- Zheng HH, Keith JM (2004) *Catal Today* 98:403
- Trichard JM (2007) *Stud Surf Sci Catal* 171:211
- Madia G, Elsener M, Koebel M, Raimondi F, Wokaun A (2002) *Appl Catal B* 39:181
- Odenbrand CUI (2008) *Chem Eng Res Des* 86:663
- Kröcher O (2007) *Stud Surf Sci Catal* 171:261
- Kapteijn F, Singoredjo L, Andreini A, Moulijn JA (1994) *Appl. Catal. B* 3:173
- Singoredjo L, Korver R, Kapteijn F, Moulijn JA (1992) *Appl Catal B* 1:297
- Smirniotis PG, Pena DA, Uphade BS (2001) *Angew Chem Int Ed* 40:2479
- Wu Z, Jiang B, Liu Y, Zhao W, Guan B (2007) *J Hazard Mater* 145:488
- Qi G, Yang RT (2003) *J Catal* 217:434
- Qi G, Yang RT (2003) *Chem Commun* 2003:848
- Qi G, Yang RT (2003) *Appl Catal B* 44:217
- Qi G, Yang RT, Chang R (2003) *Catal Lett* 87:67
- Eigenmann F, Maciejewski M, Baiker A (2006) *Appl Catal B* 62:311
- Li Y, Cheng H, Li D, Qin Y, Xie Y, Wang S (2008) *Chem Commun* 2008:1470
- Casapu M, Kröcher O, Mehring M, Nachttegaal M, Borca C, Harfouche M, Grolimund D (2010) *J Phys Chem C* 114:9791
- Chen L, Li J, Ge M (2010) *Environ Sci Technol* 44:9590
- Casapu M, Bernhard A, Peitz D, Mehring M, Elsener M, Kröcher O (2011) *Appl Catal B* 103:79
- Shan W, Liu F, He H, Shi X, Zhang C (2011) *Chem Commun* 47:8046
- Verdier S, Rohard E, Bradshaw H, Harris D, Bichon Ph, Delahay G (2008) *SAE Technical Paper Series* 1:1022
- Putluru SSR, Riisagar A, Fehrmann R (2009) *Catal Lett* 133:370
- Patil KC, Aruna ST, Mimani T (2002) *Curr Opin Solid State Mater Sci* 6:507